Tuijin Jishu/Journal of Propulsion Technology
ISSN: 1001-4055
Vol. 47 No. 02 (2026)

Geometry-driven Inventory Shrinkage and Storage Asset Selection for Natural Gas Liquids: A Techno-Economic Evaluation

Idongesit Effiong Ekpo[1*], Gideon Mudiaga Efetobor[2], Ozioma Achugasim[3], Pereware Adowei[4], Remy Uchachukwu Duru[5]

[1,3,4,5] Department of Pure and Industrial Chemistry, Faculty of Science, University of Port Harcourt, Nigeria

[2] Department of Chemical/Petroleum Technology, University of Port Harcourt, Nigeria

Abstract:- Natural gas liquids (NGLs) experience storage observed apparent shrinkage through volatilization and vapor-space dynamics, reducing saleable yield and degrading inventory integrity. In this study, a short storage period of 7 days and triplicate runs were used to assess the retention of NGL in storage vessels with varied geometries (conical, vertical cylindrical, horizontal cylindrical, cuboidal, spherical), under short-duration, bench-scale, atmospheric screen conditions identical to monitored ambient laboratory conditions (25–31 °C). Readings from the daily manual innage process were used to produce shrinkage curves and cumulative losses. From the third through the seventh day, a slower geometry-dependent loss regime was observed. On the seventh day, retained fractions of 0.384 and 0.186, for conical and spherical vessels, respectively, were obtained. The first 24 hours accounted for ~60–84% of the week-long loss. A scale-independent levelized loss indicator measured in United States dollars per liter per day ranked conical (0.0146) best and spherical (0.0192) worst. Physical loss was translated into production-economics evidence, laboratory loss fractions were annualized for a 1,600 bbl/d NGL facility, and priced at $26.29/bbl. Annual retained revenue ranged from $5.89M/yr (conical) to $2.85M/yr (spherical), implying $3.04M/yr additional retained sales value for conical storage relative to spherical. Metrics for capital recovery were applied to three dewpointing pieces of equipment, which gave payback periods of 0.226–0.758 years and return-on-investments (ROIs) of 132–443%. The data generated showed vessel geometry as a first-order lever for shrinkage mitigation, retained-value capture, and provided metrics for storage asset selection and operating policies.

Keywords: Natural gas liquids, storage shrinkage, evaporative loss, vessel geometry, exposed area, area-to-volume ratio, inventory loss, techno-economic assessment, feasibility.

1. Introduction

Natural gas liquids (NGLs) are light hydrocarbons in the C_2+ range—mainly ethane (C_2H_6), propane (C_3H_8), normal butane and isobutane (C_4H_{10}), and "pentanes plus" (≈C_5H_{12} and heavier). NGLs sit at the gas-liquid boundary and are mainly paraffins. The composition of alkanes present in the mixture determines its physical state and phase conditions with varied vapour-pressure values (U.S. Environmental Protection Agency, 2023).

Natural gas liquids contain more carbon atoms than methane and have a higher heating value, making them economically valuable; they are usually separated and sold as distinct products. (U.S. Energy Information Administration, 2023a).

In upstream gas processing, NGL recovery is mainly phase-equilibrium engineering rather than chemical reaction: the gas is treated and conditioned so that heavier hydrocarbons cross the hydrocarbon dew point and condense. Stored NGL in this study was received from processing plants, where water and non-hydrocarbon compounds were removed, and the NGL separated from the gas stream. Downstream the NGL production line, the mixed NGL stream can be fractionated into purity products (e.g., ethane, propane, butanes, pentanes-plus) (Noaman and Ebrahiem, 2021).

Industrial NGL recovery commonly uses low-temperature separation approaches based on Joule–Thomson expansion, turbo-expansion (cryogenic), or mechanical refrigeration. The workability of these methods is achieved by lowering the temperature (and changing pressure) to move the gas across its phase envelope so that C_2+ hydrocarbons condense and can be separated, improving dew-point control and generating valuable liquid byproducts. (Shoghl *et al.,* 2022; Shamsi *et al.,* 2024).

Generally, multiple mechanisms, such as:

(i) evaporation of light-end hydrocarbons,

(ii) volume reduction due to thermophysical effects, and

(iii) inventory/measurement error, influence shrinkage, but the operational consequences remain the same, causing less saleable liquid and higher reconciliation errors (Badings & van Putten, 2020; Tabari et al., 2020; de Souza Filho *et al.,* 2021).

In management accounting, shrinkage is a direct loss of product value and causes uncertainty. Modest percentage losses become financially significant at scale (de Souza Filho *et al.,* 2021). Also, Safety concerns are of the essence, as vapor-phase release of volatile hydrocarbons into flammable atmospheres can lead to environmental consequences; volatile organic compounds can accumulate, affecting compliance costs and operational risk (U.S. Energy Information Administration, 2023a; Zinke *et al.,* 2020; Jindamanee *et al.,* 2025).

The key physical drivers of evaporation-dominated shrinkage are collectively known to be volatility of substances, venting integrity, temperature history, headspace renewal, and measurement method. Also, vessel geometry may be added to the list. The exposed liquid surface governs the rate at which volatile components escape from the liquid under ambient conditions, as influenced by vessel geometry, the headspace volume, and the characteristic lengths that control heat and mass transfer (Mansour *et al.,* 2020).

As stated earlier, previous works attribute evaporative-shrinkage mostly to storage-loss physics and emissions. This study translates comparative retention behavior of NGL into screening-level production economics indicators for storage asset selection under clearly stated scale-up limits (U.S. Energy Information Administration, 2024; Shabani *et al.,* 2021; Orsay and de Oliveira, 2025).

The following are the research objectives:

(i) Measurement and comparison of data generated from volume retention of NGL samples stored in five different storage vessels with varied geometries for a period of seven days.

(ii) Shrinkage behaviour will be related to the provided geometry descriptors, focusing on exposed-area proxies.

(iii) To evaluate economic feasibility by converting shrinkage volumes into economic metrics such as value loss, levelized loss per liter per day, as well as sensitivity to price and storage duration, to support vessel selection.

2. Background

Natural gas liquids (NGLs), often reported in energy statistics as hydrocarbon gas liquids (HGLs) are light hydrocarbons that exist as gases at atmospheric pressure but can be stored as liquids under higher pressure and cooling (U.S. Environmental Protection Agency, 2023).

NGLs create value across the process and industrial material flow from upstream processing through midstream logistics to downstream utilization, and NGLs are economically strategic because they serve as petrochemical feedstocks, fuels, and blending/diluent components, Consequently, NGL management is not only a chemical-engineering matter but also a production-economics issue: losses at any node of the flow cycle reduce saleable yield, tighten supply availability, and increase unit cost.

The composition of NGLs from an upstream processing standpoint indicates a mixture of fluids with high vapour pressure. So, NGLs management, from production through storage to the point of sale, requires a strategic storage

plan to reduce operational buffers in the supply chain. To buttress the buffering role, any shrinkage during storage affects not only direct product yield but also dispatch planning, inventory availability, and downstream service levels.

Hydrocarbon shrinkage during storage is commonly driven by evaporation, flashing, and vapor displacement ("breathing") associated with ambient temperature changes and pressure dynamics. The work of Shoghl *et al.* (2022) on petroleum liquids showed that evaporation losses are strongly influenced by vapor pressure, liquid composition, and temperature, and that these losses matter commercially because they reduce recovered volume and revenue. Tabari *et al.,* (2020), inferred that Field-oriented volatile organic compound (VOC) inventory studies reinforce the same mechanism by quantifying substantial evaporative emissions from storage tanks and linking them to operational conditions and the volatility of light components. The dominant sources of VOC in storage tanks are light alkanes (e.g., pentane-class compounds), being the greatest contributor; a pattern consistent with volatility-driven liquid-to-vapor transfer. For NGL containing a large fraction of highly volatile components, the physical and chemical drivers imply that even small daily losses can compound into meaningful shrinkage over typical holding periods.

In production economics, shrinkage creates a gap between the quantity expected in inventory records and the quantity physically available for sales as well as downstream processing. It is worthy of note that inventory record inaccuracy mismatch between recorded and physically available inventory can degrade performance and cause revenue losses via poor replenishment or service failures. Therefore, strategic management is relevant to process industries so as to commit to effective planning and coordinate the processes of custody transfer, reconciliation, and production planning (including decisions on design of storage systems) to depend on accurate inventory and minimize physical losses.

A practical lever for reducing shrinkage is storage-vessel geometry, because geometry influences exposed liquid–vapor interface, characteristic transport lengths, and headspace dynamics (U.S. Energy Information Administration, 2023b).

Table 1: Comparison of academic studies relating to evaporation-driven shrinkage and inventory management

Study	Methodology adopted	Relevant findings	Commentary
Carlier and Papalexandris (2024)	- Performed direct numerical simulations (DNS) of a two-phase air–water system in a cuboidal cavity with liquid water below and an air–water-vapor mixture above, separated by an evaporating free surface. - The bottom wall was uniformly heated, which drove natural convection in both the liquid and gas layers while evaporation occurred at the interface.	- The water side forms a single-roll LSC, while the gas side forms single- or dual-roll LSCs depending on the geometry/aspect ratio. - After an initial transient, the free-surface temperature and the evaporative mass flux become approximately stabilized, but still show small temporal fluctuations due to turbulence.	- Even though the paper is air–water (not organic fluids), it is highly relevant to evaporation-dominated shrinkage because it isolates the physics that also governs many tank losses: Headspace convection matters, coupled interface dynamics, stable average loss with fluctuations, practical scaling handle, and moving free surface (real shrinkage)
Mansour et al. (2020)	-The authors reported collecting 44 samples from different hydrocarbon storage tanks, with variation in tank height (H2) and sampling point height (H1) to reflect how location within a tank can affect measured properties and losses.	- Concluded that evaporation/flashing from storage tanks is an important product-loss pathway. - Proposed a new empirical equation intended to reduce "human errors" in manual	- Their "flashing loss" is essentially a shrinkage mechanism—volume reduction caused by liberation of dissolved gas/light ends when pressure drops to near-atmospheric conditions. -- This is directly relevant to NGL/condensate storage where light components

Study	Methodology adopted	Relevant findings	Commentary
		estimation while using readily available field/lab variables.	and temperature can amplify losses.
Poós (2020)	- Investigated water evaporation under forced convection (air flowing over an unheated water surface), varying air velocity and air temperature. - Laboratory apparatus was used to measure evaporation rate directly (by tracking water mass loss over time) under controlled airflow/temperature conditions. - They computed the mass transfer coefficient using one theoretical method and ten empirical correlations gathered from the literature, then compared the resulting coefficients as a function of air velocity and temperature.	- Evaporation rate increases with air velocity and air temperature (for water without heating). - Among the empirical correlations tested, the Inan and Atayilmaz correlation yielded mass-transfer coefficient results closest to those from the theoretical method, as supported by Bland–Altman agreement analysis. - This allowed them to extend the applicability range of that empirical equation for combinations of water temperature, air temperature, air velocity, and relative humidity covered by their experiments.	- Even though the study is water–air (not hydrocarbons), it is directly useful for interpreting evaporation-dominated shrinkage in storage tanks: Increase in air velocity increases evaporation; supports the storage-tank idea that gas-phase mixing/renewal above the liquid (from wind, thermal convection, or venting) can raise shrinkage rates by maintaining a strong vapor-concentration driving force. - Their finding that increasing air temperature increases evaporation is consistent with the fact that storage behaviour where warmer ambient conditions typically elevate vapor pressure and loss tendency—especially relevant for volatile liquids.
Shabani *et al.* (2021)	- >5,250,000 inventory items across 81 stores from an international fashion retailer were retrieved and used as real-life retail data. - An evaluation of Inventory record inaccuracy (IRI), the mismatch between recorded inventory (QR) and physically available inventory (QP), was carried out.	- Their computational experiments showed the benefit of using relative measures to quantify IRI more accurately across stock-keeping units (SKUs), and that doing so supports better identification of IRI root causes. - They found negative correlations between efficiency and both IRI improvement potential (−0.717) and IRI improvement workload (−0.489), and a positive correlation between improvement potential and workload (0.864).	- They explicitly note that IRI can arise from shrinkage (such as theft, damage, or quality issues), as well as misplacement and transaction/recording errors. - In tanks, shrinkage (evaporation, leaks, or venting) creates the same kind of record physical mismatch that they defined as IRI; i.e., “book inventory” differs from what is physically available. The paper provides language and structure to justify shrinkage as both a value loss and an inventory integrity problem.
Tabari et al. (2020)	- 36 storage tanks at a large petroleum and chemical export terminal in southwest Iran; with 32 external floating-roof tanks (EFRTs) and 4 internal floating-roof tanks (IFRTs) treated as 36 point sources across about 3.8 km², with emissions evaluated over 12 months. - VOC emission rates were calculated using US EPA	- Estimated total VOC emissions from the tank farm were 881.74 tons/year, with EFRTs contributing 865.7 tons/year (98.18%) and IFRTs 16.04 ton/year (1.81%). - The highest VOC emissions occurred in July, coinciding with the highest temperature and wind speed.	- The study quantifies evaporative VOC losses, which are essentially the mass-loss component of shrinkage (liquid molecules leaving the stored product as vapor). - There is a practical shrinkage implication: deck fittings and seals dominate emissions support. Even with the same stored liquid, hardware integrity and sealing

Study	Methodology adopted	Relevant findings	Commentary
	TANKS 4.0.9d, which estimates emissions from surface evaporation of organic liquids in storage tanks. Thermodynamic/fluid data were supported using Aspen HYSYS, and meteorological inputs (e.g., daily temperatures/pressure, solar radiation, wind speed) were entered into tanks.	- The highest VOC emission rate was attributed to light naphtha tank No. 67 (56.73 ton/year) and the lowest to a jet naphtha tank (4.18 ton/year); for BTEX, the highest and lowest reported were 0.37 and 0.05 ton/year, respectively.	quality can strongly affect volume retention, which is important when interpreting shrinkage curves and proposing mitigation options.
Varju and Poós (2022)	- A new dimensionless (Sherwood-based) correlation for evaporation from an open liquid surface under natural convection, focusing on steady-state gas and liquid conditions, was developed. - Instead of running new experiments, they compiled evaporation measurements from prior literature that reported sufficient supporting data, then used those datasets to build/regress a correlation.	- Compared with existing correlations for natural-convection evaporation, their new dimensionless equation matched the measurement datasets best, with an average relative error of ~9.5%. - The work emphasizes that evaporation in natural convection is strongly influenced by thermophysical properties, temperature/humidity, pressure, and container characteristic length, not just a single "area × vapor-pressure" term.	- In storage tanks, shrinkage due to evaporation is essentially a mass-transfer problem at the liquid–vapor interface. This paper is useful because it provides a decision-ready approach to connect the evaporation rate to geometry (via an equivalent characteristic length) and to the headspace driving force (via partial vapor pressures and total pressure).
This Study	- Innage measurement of loss and retained volume of NGL in storage vessels with varied headspaces was carried out. - The storage vessels were designed with the led-down methodology, and their void areas were determined. - The storage inventory was translated into production-economic models, which inform the production management discussion in the study.	- This study will contribute to a framework that links shrinkage behaviour to exposed area and to economic impacts, so as to enable rapid screening of vessel options for short-term NGL storage.	- The variation in the magnitude of head spaces created by the varied geometry of the storage vessels to evaporative-shrinkage will be checked, as well as the rate of volume losses to void areas. - The experimental amounts of loss volume and the economically converted value will be used to show the reason for the mitigation of evaporative shrinkage.

3. Method

3.1 Experimental Setup and Procedure

The experimental setup for this study involved a common-ambient screening test, in which an NGL sample from a single batch was stored in five different storage vessels under controlled ambient laboratory conditions for 7 consecutive days (Day 1–Day 7) to quantify short-term shrinkage under near-field storage conditions. A 1000 mL volume of the NGL sample was filled in each vessel with the same closure and venting conditions. Estimation of the shrinkage pattern involved measuring the volume remaining at a fixed time each day to generate shrinkage curves and estimate daily and cumulative loss rates. Ambient temperature was monitored throughout the test and remained within 25–31°C.

Each vessel was cleaned, dried, and weighed before filling; measurements were made using the same instrument and reading protocol. The vessels with contents were kept away from direct sunlight and local heat sources to minimize radiative heating and non-uniform thermal loading.

All vessels were collocated in the same laboratory environment and handled using an identical protocol so that differences in shrinkage could be attributed primarily to geometry exposure characteristics (example, exposed-area proxies and characteristic length effects on heat/mass transfer). The data collection for all vessels was in triplicate.

3.2 Design of Storage Vessels

The storage vessels used in this study were fabricated as bench-scale vessels in five geometries to express the effect of evaporation rate on void space in vessel geometry on measured liquid shrinkage.

Regardless of the fact that the vessels were made from small containers with different geometries, the design philosophy was based predominantly on the standards for storage tanks, with an emphasis on integrity, dimensional control, and safe containment of liquids (American Petroleum Institute, 2020; American Society of Civil Engineers, 2022). As a global best practice, the required capacity and hold-up volume were considered the primary sizing parameters before detailing the geometry and fabrication requirements. So, the storage vessels were produced with a volume of 1.5 ± 0.2 L, which enabled vessels that align with sufficient liquid volume so as to withstand repeated volume measurements and comparability of shrinkage trends across geometries under identical ambient conditions. (American Society of Civil Engineers, 2022). Vertical cylindrical, Horizontal cylindrical, spherical, conical, and Cuboidal vessels were designed using 2D fabrication drawings and 3D Computer-Aided Design (CAD) models. Autodesk AutoCAD was used for the vessel's design. (Autodesk, 2024; García-G et *al.,* 2024).

3.3 Tank Volume Measurement to Determine Shrinkage

Liquid quantity in each vessel was determined from the measured liquid level (depth) and a vessel-specific calibration chart (capacity table). In manual dipping, a calibrated rule/tape was lowered to a fixed reference (datum), and the wetted line indicates the liquid level; the innage gauge method here could also be referred to as manual dipping. The observed level was then converted to volume using the capacity table prepared for that vessel. This approach follows established manual tank-gauging practice for petroleum and related liquids **(**American Petroleum Institute, 2021; International Organization for Standardization, 2023). After transfer, each vessel was allowed to stand briefly to minimize sloshing and to obtain a stable free surface before gauging (important for repeatable level readings).

Consistent reference-point control was enhanced as all depth readings were taken to the exact vessel bottom. This was critical because any "zero-offset" between the gauging reference and the calibration table reference introduces systematic bias in volume results.

A thin, uniform layer of oil paste was applied to the lower portion of the rule/tape over the expected wetting zone.

The measuring tape was lowered vertically until the bob just reached the bottom of the vessel.

The measuring tape was carefully withdrawn, and the measurement of the sharp change in the paste (wetted boundary) was read as the innage depth (h) to the nearest graduation.

Manual gauging steps and key influences (reference point, tape handling, bob effects) are consistent with recognized petroleum manual-gauging guidance.

The readings were taken in triplicate (without changing the reference point), and the mean depth was recorded as the daily level for all vessels.

Measured depth (h) was converted to volume (V) using the vessel-specific capacity table/calibration chart developed for each geometry. Capacity tables are the standard mechanism for translating gauged levels to contained volumes.

Before shrinkage monitoring, each vessel geometry was calibrated to establish the relationship between measured liquid level (h) and contained volume (V). Practically, this was done by stepwise addition of known volumes and recording the corresponding depths to generate a lookup table or fitted function $= f(h)$. International calibration standards emphasize documenting the calibration method and using the resulting capacity table to determine volume at gauged levels (International Organization for Standardization, 2022; International Organization for Standardization, 2023).

Daily shrinkage was calculated as the fraction of the volume change ($\Delta V_t = V_o - V_t$) relative to the initial volume (V_o), as shown in Equation 1. The linear model and exponential model to estimate the volume loss and remaining fraction are presented in Equation 2 and Equation 3, respectively, and Equation 4 shows the expression for the levelized loss (LL) (Huang *et al.,* 2020).

$$\%\text{shrinkage}_t = \frac{V_0 - V_t}{V_0} \times 100 \quad (1)$$

$$V_t = V_0 - K_L t \quad (2)$$

$$V_t = V_0 e^{-K_E t} \quad (3)$$

$$LL = \frac{\sum_{t=1}^{r} (\Delta V_t \times P)}{V_0 \times T} \quad (4)$$

Where V_o is the initial volume of liquid in the vessel in liters

V_t is the volume of liquid left in the vessel after evaporation at the period of

Measurement in liter

K_L and K_E are the constants for the linear model and the exponential model, respectively.

LL is the levelized loss in US$/L-day

ΔV_t is volume loss at time t

P is the unit price of NGL in US$/L

T is the total storage time in days

3.4 Economic Feasibility Model

3.4.1 The Process Economics

The study is considered for a natural gas well with 20,000 Mcf/d gas production, having a moderately rich natural gas stream of about 3.36 GMP (gallons of NGL per Mcf of gas processed), which is equivalent to 1,600 bbl per day of NGL (from Equation 5), with gross value approximately $26.29/bbl NGL (EOG Resources, Inc., 2025; U.S. Energy Information Administration, 2026). According to Verret *et al.* (2024), the capacity correlation to estimate purchase equipment cost by applying the given cost exponent and the six-tenth rule is as shown in Equation 6. Considering Joule–Thomson expansion, turbo-expansion (cryogenic), and mechanical refrigeration fitted with an export compressor (for transferring produced pipeline natural gas) to have the screening capital expenditure (CAPEX) is $ 4.5 M, $ 6.5 M, and $ 4.0 M at 10,000 bbl/day NGL production capacity, respectively. The exponent constant of 0.60 for these equipment types will yield CAPEX estimates of $1.50M, $2.16M, and $1.33M, respectively, for these three pieces of equipment, estimated at 1,600 bbl/day NGL production capacity.

The recovered NGL from processing is often produced as a mixed stream (“Y-grade”) that is then separated by fractionation into purity products (ethane, propane, normal butane, isobutane) and pentanes plus, depending on facility configuration.

$$V_{NGL}\ (\text{bbl/d}) = \frac{GPM \times V_N}{42} \quad (5)$$

Where:

V_{NGL} is the volume flow rate of NGL produced in a day (bbl/d)

GPM is the gallons of NGL per Mcf of gas processed (Mcf/d)

V_N is the volume flow rate of the natural gas processed from the hydrocarbon well.

$$\frac{C_a}{C_b} = \frac{(A_a)^n}{(A_b)} \quad (6)$$

Where:

C_a is the evaluated CAPEX for equipment

C_b is the CAPEX for similar equipment at known capacity.

A_a is the operating capacity of the evaluated equipment.

A_b is the operating capacity of similar equipment with known capacity.

n is the cost exponent for shell and tube stainless steel exchanger per unit area.

3.4.2 Boundary and Scenario Definition

In this study, the volume of NGL loss after 7 days was experimentally measured and used as an economic indicator to determine the extent of economic loss based on the storage vessel geometries. Lifting from The Open University (2026), the cash flow principle followed is that where only cash flows that change between the baseline and storage cases are included, and CAPEX is treated for the recovery process equipment (sunk costs excluded).

This study defined the following two (2) economic scenarios:

- Baseline (no storage): NGL produced and sold in real time, with no storage-related shrinkage. Accordingly, the baseline shrinkage cost is taken as $CUMC_{baseline} \approx 0$.
- Option (with storage): NGL stored for seven days in each of the five vessel geometries (conical, vertical cylindrical, horizontal cylindrical, cuboidal, spherical) under the same ambient conditions, resulting in measurable shrinkage (volume reduction).

The analysis boundary is limited to direct product value loss due to shrinkage during storage.

3.4.3 Shrinkage Valuation and Cumulative Monetary Cost

For each vessel geometry, the cumulative monetary cost ($CUMC_t$) of shrinkage over the observation window was computed as in Equation 7.

$$CUMC_t = (V_0 - V_t) \times P \quad (7)$$

Where:

$CUMC_t$ is the cumulative value loss for seven days and extrapolated to 1 year in $

V_o is the initial volume of liquid in the vessel in Liter

V_t is the volume of liquid left in the vessel after evaporation at the period of

measurement in Liter

P is the unit value of NGL in $/Liter

3.4.4 Annualization of Shrinkage Cost

To express the economic impact on an annual basis, the seven-day shrinkage cost was extrapolated to one year using an annualization factor (N), as shown in Equation 8. This was further used to evaluate the annualized storage shrinkage cost (Equation 9) defined as the number of equivalent storage cycles per year (Equation 8).

The annual economic penalty of storage shrinkage (S_{annual}) is then derived from Equation 9 as shown in Equation 10.

$$N = \frac{365}{7} \quad (8)$$

$$CUMC_{\text{option,annual}} = N \times CUMC_{\text{option,7d}} \quad (9)$$

$$S_{\text{annual}} = CUMC_{\text{baseline}} - CUMC_{\text{option}} \quad (10)$$

Where:

S_{annual} is the amount of money saved in an ideal situation where NGL are sold at real

time at within a period of one year in $, and other parameters remain as described earlier.

Given $CUMC_{\text{baseline}} \approx 0$, S_{annual} is negative and is interpreted as the economic penalty within one year (annually). For investment indicators that require a benefit term, the loss magnitude is expressed as in Equation 11 (Lake, 2026; Vipond, 2026).

$$S_{\text{annual,loss}} = -S_{\text{annual}} = CUMC_{\text{option,annual}} \quad (11)$$

This keeps the directionality explicit (storage shrinkage reduces saleable value) while enabling consistent payback and ROI reporting (EFFECT4buildings, 2026).

3.4.5 Payback and ROI indicators using incremental CAPEX

Incremental CAPEX represents the additional capital required for the storage option (or for the equipment or asset choice being evaluated) relative to the no-storage baseline, consistent with the exclusion of sunk costs. A payback-type (PB) indicator was computed from Equation 11, as shown in Equation 12 (National Renewable Energy Laboratory, 2026).

$$PB = \frac{CAPEX}{S_{\text{annual,loss}}} \quad (12)$$

The number of years of shrinkage losses that are equivalent to the incremental investment (i.e., how quickly shrinkage can "erode" the investment value). This is consistent with the standard definition of payback as the time required for cumulative annual effects to match the upfront cost. An ROI-type indicator was computed as in Equation 13 (Lake, 2026).

$$ROI_{\text{annual}} = \frac{S_{\text{annual,loss}}}{CAPEX} \quad (13)$$

The fraction of incremental CAPEX effectively "lost per year" due to shrinkage (an ROI penalty), grounded in the standard ROI concept of net gain/loss relative to invested cost.

3.5 Statistical analysis

The vessel geometry mean, standard deviation, range, coefficient of variation, and 95% confidence intervals were used to summarize daily NGL retained volume, cumulative loss, annualized loss cost, payback period, and ROI. A repeated-measures ANOVA was used to test vessel effects on cumulative loss, since the seven-day observations constitute repeated measurements within each vessel. Shapiro–Wilk tests normality, and Levene's tests assess homogeneity of variance, Mauchly's test assesses sphericity, and violated assumptions were fixed with a Friedman rank test. Post-hoc comparisons were conducted using Tukey HSD after an ANOVA test with Holm adjustment and after Friedman analysis, with significance accepted at adjusted $p < 0.05$.

Economic indicators were analysed descriptively because they were derived deterministically from loss fractions, with annual value loss ranging from US$9.46 × 10⁶/yr to US$12.50 × 10⁶/yr.

4. Findings

4.1 Deduction from Shrinkage Curves

Fig. 1 shows the volume of NGL remaining in millilitres versus the day of measurement for the NGL stored in each vessel geometry. All geometries exhibited a rapid initial decline between Day 1 and Day 2, followed by a

slower, geometry-dependent decline through Day 7. This pattern is consistent with an early, strong driving force for the evaporation of light ends and rapid attainment of equilibrium between the liquid and headspace, after which the net loss rate decreased as the system approached a lower-volatility state, as shown by nearly flat plots from Day 5 to Day 7.

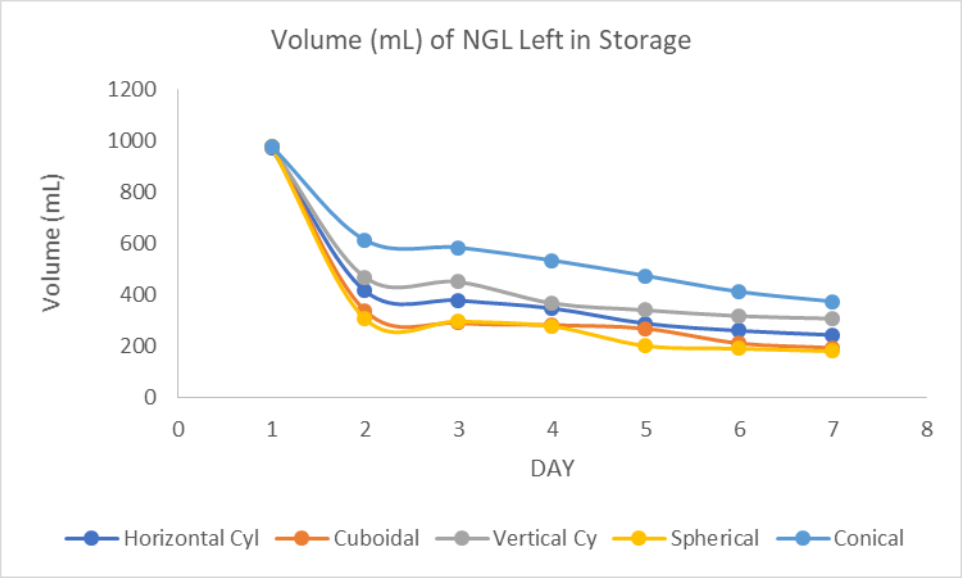

Figure 1. Amount (mL) of NGL left in different storage vessels after daily evaporation

4.2 Geometry Ranking and Retention Performance

Across the seven-day monitoring period, the conical vessel exhibited the highest volume retention, while the spherical vessel exhibited the lowest. This outcome is directionally consistent with the exposed free-surface area (A_e) reported in Table 2: the conical vessel has the smallest estimated exposed area ($A_e \approx 36$ cm^2), whereas the spherical and vertical cylindrical vessels have substantially larger free-surfaces (≈ 804 cm^2 and ≈ 707 cm^2, respectively). So, the stated rank in area (A_e) from small to large was deduced as: Conical < Cuboidal < Horizontal < Vertical < Spherical.

A practical ranking based on end-of-test retention (Day 7) as a first-order descriptor is: Conical (best retention) > Vertical cylindrical > Horizontal cylindrical > Cuboidal > Spherical (lowest retention). The changes in the intermediate order for the rank in area and end-of-test retention here indicate that the exposed area (the liquid-vapour interface) alone is insufficient to predict shrinkage patterns. However, the conical and spherical outcomes support the expectation that a smaller exposed interface is beneficial for retention. In particular, the vertical cylindrical vessel retained more volume than the horizontal cylindrical and cuboidal vessels, despite having a larger A_e, suggesting that additional controlling factors, such as headspace volume, vapor renewal conditions, sealing or closure effectiveness, vessel orientation, and wall wetting or film formation, also play a role. From these findings, it can be deduced that phase transport resistance, which governs the net loss, collectively contributes to the effective evaporating area.

4.3 Relationship Between the Exposed area and Shrinkage Behaviour

The results suggest that the exposed free-surface area (A_e), Table 2 is a useful first-order descriptor, especially for distinguishing the best- and worst-performing geometries. Specifically, the smallest A_e case (conical) produced the highest retention, and the largest Ae case (spherical) produced the lowest retention; this supports the general expectation that shrinkage caused by evaporation increases with available liquid–vapor interfacial area under comparable ambient conditions.

However, the relationship is not strictly monotonic across all vessels, suggesting that shrinkage is governed by multi-parameter geometric effects rather than by exposed area alone. From a transport standpoint, the net

evaporative loss rate depends on: (i) the effective interfacial area, (ii) the driving force due to components of the mixture and temperature, and (iii) the gas-phase transport resistance in the headspace and near the interface. Vessel geometry influences these terms by shaping the free surface, modifying natural convection/mixing patterns in the headspace, and—where openings are restricted—limiting vapor exchange with the surrounding environment.

Table 2: Estimated liquid-vapour interfacial area (Ae) at 1000 mL fill storage vessels

S/N	Vessel type	Liquid surface shape	Equation for calculation of A_e	Estimated free-surface area (A_e) (cm^2)
1	Spherical	Circle	$\pi(2rh-h^2)$	804
2	Vertical Cylindrical	Circle	$\pi \frac{D^2}{4}$	707
3	Horizontal cylindrical	Rectangle	$2L(h(D-h))^{1/2}$	228
4	Cuboidal	Rectangle	LB	185
5	Conical	Circle	$\pi r(h)^2$	36

r is the opening radius; D is the diameter; h is the height; L is the length, and B is the breadth, all were measured to compute the exposed free-surface footprint at the 1000 mL fill mark; dimensions were measured to ± 0.2 cm.

4.4 Cumulative Volume Loss Dynamics

Table 3 shows cumulative shrinkage as $V_0 - V_t$ (L) for each vessel, for a period of seven days. It could be observed that this accumulates daily losses into a single running total, it is particularly useful for production-economics interpretation; this signifies lost saleable inventory, inventory record inaccuracy, and reconciliation burden at the end of a holding period.

4.4.1 Dominant Early-loss Interval and Subsequent "Slowdown"

It is observed that a dominant early-loss interval and subsequent slowdown, shown by the large jump from Day 1 to Day 2 across all vessels. The cumulative losses already reached on Day 2:

- Conical: 0.365 L
- Vertical cylindrical: 0.508 L
- Horizontal cylindrical: 0.554 L
- Cuboidal: 0.640 L
- Spherical: 0.672 L

Comparing this to the total volume of NGL in Day-7 left in the vessels, this indicates that the first 24 hours account for most of the week's shrinkage, especially for higher-loss vessels:

- Conical: 0.365/0.604≈60%
- Vertical cylindrical: 0.508/0.669≈76%
- Horizontal cylindrical: 0.554/0.726≈76%
- Cuboidal: 0.640/0.785≈82%
- Spherical: 0.672/0.798≈84%

Operationally, these two observed periods of evaporation are consistent with a rapid initial depletion of the most volatile fraction and rapid equilibration with headspace conditions, followed by a slower, more incremental loss period observed for Days 2–7. For production planning, this means that delays in the choice of storage, to reduce

shrinkage by evaporation can create short-term losses, because from this study, the marginal loss rate is highest early in the storage system.

4.4.2 Geometry-dependent Cumulative Loss Ranking

By the end of the monitoring period (Day 7), Table 3 shows a clear ranking in cumulative loss:

Conical < Vertical Cyl < Horizontal Cyl < Cuboidal < Spherical.

The findings:

- The conical vessel consistently delivers the lowest cumulative loss on every day after Day 1.
- The spherical vessel remains the worst performer, with the highest cumulative loss throughout the period.
- The magnitude of this effect is practically meaningful. By Day 7, the conical vessel reduced cumulative loss relative to the spherical vessel's cumulative loss; ~24% reduction relative to the spherical vessel's cumulative loss. Cuboidal: 0.785-0.604 = 0.181L, less loss ~23% reduction relative to the cuboidal vessel's cumulative loss, ~17% reduction relative to the horizontal cylindrical vessel's cumulative loss,
- Vertical cylindrical: 0.669−0.604=0.065 L less loss and ~10% reduction relative to the vertical cylindrical vessel's cumulative loss.

4.4.3 Diminishing Incremental Losses after the First Day

Although spherical and cuboidal vessels exhibit the largest total cumulative losses, their incremental losses after Day 2 are smaller than those of the conical vessel. For example, from Day 2 to Day 7:

- Conical with +0.239 L increment from 0.365 to 0.604 L
- Spherical with +0.126 L increment from 0.672 to 0.798 L
- Cuboidal with (+0.145 L) increment from 0.640 to 0.785 L

These show that the capacity to contain the stored fluid is not only “less loss,” but also less extreme early loss, which matters for operational reliability.

The production and distribution systems can utilize Table 3 as an inventory integrity indicator, as cumulative shrinkage is not just a physical loss; it introduces uncertainty into:

- Available-to-promise quantities; clarifying quantity that can be shipped versus recorded quantity,
- Reconciliation of custody transfer and
- Causes risk of short deliveries when inventory is assumed to be intact.

Delaying dispatch by even a day can create disproportionate reconciliation gaps, because losses are largest early in storage; Figure 2 showed that conical, vertical cylindrical, horizontal cylindrical, cuboid and spherical vessels had total percentage of NGL loss as 61.0, 68.40, 74.80, 80.10 and 81.40 %, respectively. This may support the use of geometry selection factored into associated liquid and vapour interface, as well as transport characteristics as an operational lever to reduce inventory errors caused by shrinkage and protect material flow performance.

Table 3: Cumulative volume loss (L) of NGL by vessel ($V_0 - V_t$)

Day	Conical (L)	Vertical Cyl (L)	Horizontal Cyl (L)	Cuboidal (L)	Spherical (L)
1	0.000	0.000	0.000	0.000	0.000
2	0.365	0.508	0.554	0.640	0.672
3	0.394	0.526	0.591	0.688	0.682
4	0.444	0.609	0.622	0.696	0.701

5	0.504	0.636	0.681	0.710	0.777
6	0.566	0.659	0.709	0.767	0.788
7	0.604	0.669	0.726	0.785	0.798

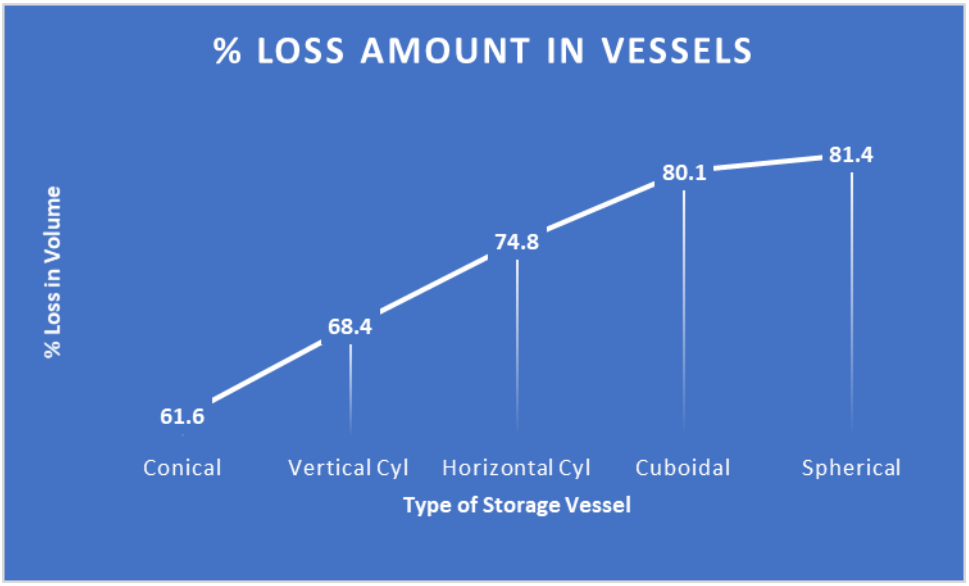

Figure 2. Percentage (%) loss of NGL in the vessels within the period of study

4.5 Shrinkage Summary and Screening Indicators

The seven-day shrinkage experiment is summarised in Table 4. Here, the outcome of shrinkage across the vessels, from the first day (V_o) to the last day (V_7), presented physical loss metrics (total loss, loss fraction, average loss rate), and two screening economic indicators ($CUMC_{7d}$, LL), which are expected to translate shrinkage into decision-ready production economics evidence.

All vessels started with almost identical initial volumes ($V_0 \approx 1000$ mL). Differences in V_7 largely reflect geometry-linked shrinkage behaviour rather than different starting inventory. End-of-test volumes show a clear ranking:

- Conical: $V_7 = 0.376$ L (best retention)
- Vertical cylindrical: $V_7 = 0.309$ L
- Horizontal cylindrical: $V_7 = 0.245$ L
- Cuboidal: $V_7 = 0.195$ L
- Spherical: $V_7 = 0.182$ L (lowest retention)

The order of volume left in vessels is consistent with the cumulative losses reported here: the conical vessel systematically minimised the loss accumulation relative to the other geometries, while the spherical geometry produced the largest end-of-period shrinkage. The order of variation retained in the vessels showed that the conical vessel retained more than the spherical vessel by approximately 0.194 L by the 7th Day. However, both volumes started with approximately 1000 mL.

4.5.1 Shrinkage Magnitude and Loss-rate Interpretation

Across the 7-day window, total losses ranged from 0.604 L (conical) to 0.798 L (spherical), corresponding to loss fractions of 0.616 to 0.814. The absolute losses of the laboratory bench-studies are hypothesized to optimize industrial pressurised vessels.

According to the work of Carlier and Papalexandris (2024), the evaporation rate is often stabilized around a mean; this study was conducted under constant environmental conditions across all vessels. So, it could be deduced that the point of stability is when the volatile components have been completely vaporized. This may be the reason the change in volume for the conical vessel is greater than that of the other vessels towards the end of the test. In Table 4, the average daily loss rate increases monotonically from conical (0.086 L/day) through to spherical (0.114 L/day). This provides a compact, manager-interpretable measure of expected loss intensity per day under the tested conditions.

4.5.2 Economic Screening Indicators: $CUMC_{7d}$ and Levelized Loss (LL)

To convert physical shrinkage into economically comparable metrics using the direct cost of the 7-day shrinkage for the ~1 L batch at the stated NGL unit value ($CUMC_{7d}$) in US$ per batch and the normalized "levelized" shrinkage-loss rate per unit inventory per unit time (LL) [US$/L-day]; used as screening indicators. The $CUMC_{7d}$ values range from $0.0999 (conical) to $0.1320 (spherical) per batch. While these absolute values are small at the laboratory scale (because the batch is ~1 L), they are economically meaningful as scalable coefficients: both $CUMC_{7d}$ and LL scale linearly with inventory size and throughput.

The levelized loss LL shows a consistent ranking that mirrors the physical performance:

- Conical: 0.014559 US$/L-day
- Vertical cylindrical: 0.016159 US$/L-day
- Horizontal cylindrical: 0.017662 US$/L-day
- Cuboidal: 0.018922 US$/L-day
- Spherical: 0.019236 US$/L-day

The explanations above show that cost-per-inventory daily can be shifted by the geometry choice, as the spherical vessel's LL is approximately 24% higher than the conical (0.019236 vs 0.014559).

4.5.3 Relevance to Production Economics

A close view of process and supply chain operations show that shrinkage reduces the amount of produced fluids available for sales and creates gap between recorded and physically available inventory.

In process and supply-chain terms, shrinkage reduces saleable output and introduces a persistent gap between "expected" and "physically available" inventory. Inventory record inaccuracy, a mismatch between recorded and physically available inventory, can impair performance and contribute to revenue losses through poor replenishment decisions and service failures (Shabani, et al., 2021).

On the other hand, the volume of NGL shrank across each vessel within the 7-Day survey. Petroleum and organic products storage tanks are abundant sources of evaporative volatile organic compounds (VOCs). So, reducing shrinkage aligns not only with revenue protection but also with loss-prevention and emissions-management objectives. It has been shown here that LL is scale-independent, directly monetizes shrinkage, and maps cleanly to annualized feasibility calculations when multiplied by operating inventory and storage days (Table 4). In application, LL with minimum geometry should be selected.

Table 4: Seven-day shrinkage summary and screening indicators (per batch)

Vessel	V_0 (L)	V_7 (L)	Total loss (L)	Loss fraction (Day 7)	Avg loss (L/day)	$CUMC_{7d}$ (US$ per batch)	LL (US$/L-day)
Conical	0.980	0.376	0.604	0.616	0.086	0.0999	0.014559
Vertical Cyl	0.978	0.309	0.669	0.684	0.096	0.1106	0.016159

Horizontal Cyl	0.971	0.245	0.726	0.748	0.104	0.1201	0.017662
Cuboidal	0.980	0.195	0.785	0.801	0.112	0.1298	0.018922
Spherical	0.980	0.182	0.798	0.814	0.114	0.1320	0.019236

4.6 Annualized shrinkage cost

Physical and loss mechanisms can be expressed as lost throughput, lost revenue, and inventory integrity penalty. This may help managers select a storage asset. In Table 5, the observed 7-Day shrinkage is converted into annualized economic exposure using the considered quantity of 1,600 bbl/day as procured equipment capacity for NGL production through dewpointing. The Day-7 loss fraction may be used as a representative practical screening assumption, and the annualized losses are intended as screening metrics that translate experimental loss fractions into operational value exposure under fixed throughput and price assumptions.

In Production economics, each column of Table 5 represents the following:

- Loss fraction (Day 7) is the fraction of the handled inventory assumed to be lost (shrinkage) after storage. It is used here as a practical "representative" factor for annual scaling.
- Annual loss (bbl/yr) translates that fraction into lost saleable barrels:
- Annualloss = (Q×365)×Loss fraction (where the barrel is the standard petroleum volume unit).
- Annual value loss (US$/yr) monetizes the annual lost barrels using the chosen unit price.
- Annual retained revenue (US$/yr) is the remaining gross value of NGL after shrinkage:
- Annual retained revenue=(Q×365×P)−Annual value loss

Table 5 shows a consistent ranking in annualized outcomes:

Conical (best) < Vertical Cyl < Horizontal Cyl < Cuboidal < Spherical (worst)

- Conical: loss fraction 0.616, annual loss 359,935 bbl/yr, annual value loss $9.46M/yr, retained revenue $5.89M/yr
- Spherical: loss fraction 0.814, annual loss 475,543 bbl/yr, annual value loss $12.50M/yr, retained revenue $2.85M/yr

Selecting the conical vessel reduces annual loss by 115,608 bbl/yr and reduces annual value loss by $3.04M/yr. That difference is significant, and it is an operationally meaningful gap once scaled to throughput and time.

A second insight is how much revenue is "kept" under each geometry relative to the no-shrinkage baseline at the same throughput. From the declared baseline annual gross value, conical retains about 38% of the baseline value, while spherical retains only about 19%. This shows that the choice of asset affects realized value capture, along with technical performance.

From a production economics perspective, shrinkage is more than lost product; it also creates a mismatch between "recorded/expected" inventory and the physical inventory available for dispatch. Mismatches between recorded and physically available inventory can degrade operational performance and lead to downstream inefficiencies and losses (Shabani *et al.,* 2021).

Also, Table 5 indicates that the least-performing vessels, such as spherical and cuboidal, in this study not only reduce saleable volume but also increase the magnitude of the reconciliation gap that planners and operators must manage.

Table 5's "annual value loss" is consistent with the broader engineering understanding that organic-liquid storage systems can experience material losses through volatilization and vapor displacement, and that the primary

pollutant of concern is volatile organic carbons (VOCs). US EPA's AP-42 (2020), guidance explicitly treats organic liquid storage tanks as emission sources and provides models to estimate emissions from them.

Table 5: Annualized shrinkage cost (using Day-7 loss fraction as representative)

Vessel	Loss fraction (Day 7)	Annual loss (bbl/yr)	Annual value loss (US$/yr)	Annual retained revenue (US$/yr)
Conical	0.616	359,935	9,462,683	5,890,677
Vertical Cyl	0.684	399,485	10,502,452	4,850,908
Horizontal Cyl	0.748	436,647	11,479,443	3,873,917
Cuboidal	0.801	467,796	12,298,355	3,055,005
Spherical	0.814	475,543	12,502,022	2,851,338

4.7 Annualized Sales Value of NGL Remaining after 7-day Storage

Using the conical vessel as the baseline (annual savings = $0/yr), the comparative results show that vessel geometry has a measurable, recurring impact on the annualized sales value of Natural Gas Liquids (NGL) remaining after a 7-day storage period that was extrapolated into 1 year of storage (i.e., evaporation-based shrinkage translates directly into lost saleable inventory value). The reported annual savings represent the difference between the annualized value of NGL sales retained in the conical vessel and that retained in each alternative vessel, as shown in Figure 3.

Annual savings of conical versus other vessels ($/yr) ranked in increasing order:

- Vertical cylindrical vessel: $1,039,769/yr
- Horizontal cylindrical vessel: $2,016,760/yr
- Cuboid vessel: $2,835,672/yr
- Spherical vessel: $3,039,339/yr

The above shows that the conical vessel had the highest NGL storage amount over the year. The spherical vessel has the highest annualized value losses relative to the conical storage vessel baseline.

Because the savings are defined as "conical minus alternative," a larger savings value implies that more NGL sales value is forfeited (via shrinkage) in the alternative vessel. The ordering of economic performance (closest to conical → farthest from conical) is therefore:

Vertical cylinder (best alternative) → Horizontal cylinder → Cuboid → Spherical (worst alternative).

Quantitatively, selecting a spherical vessel instead of a conical one corresponds to an annualized penalty of $3.04 million/yr, which is about $2.00 million/yr more loss than the vertical cylinder's penalty ($1.04 million/yr). The spherical and cuboid outcomes are relatively close (difference ≈ $0.204 million/yr); these two have comparable economic exposure.

These mechanisms are consistent with classic tank-loss discussions that identify multiple loss mechanisms and emphasize that tank design/operation materially affects evaporative behaviour.

The results have a clear managerial message: inventory yield preservation (saleable NGL retained after storage) is sensitive to asset design choices. Here, the conical vessel is the economic benchmark, and the vertically cylindrical storage vessel is the nearest substitute (lowest annualized penalty), while the spherical vessel is the highest-loss option relative to conical. This provides a direct basis for screening decisions when storage configuration is being chosen to minimize shrinkage-driven value leakage.

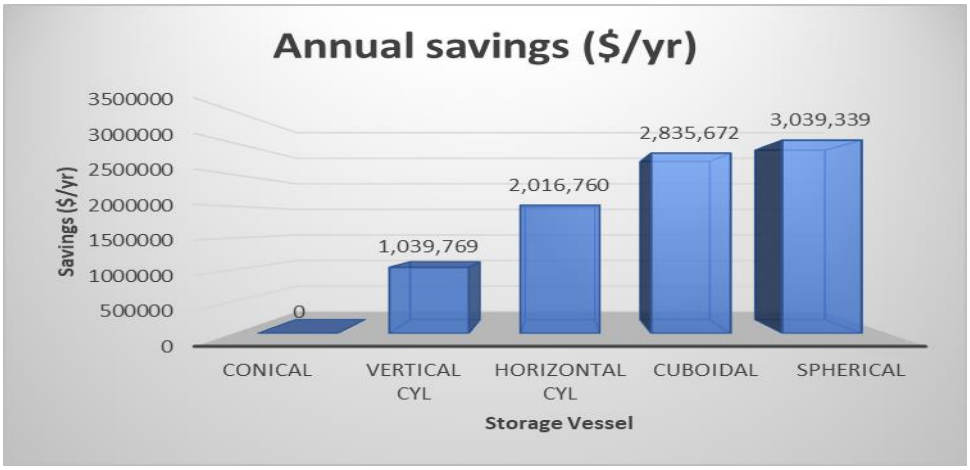

Figure 3. Comparing the annual savings ($/yr) using the conical vessel as a baseline for other vessels

4.8 Payback Period for NGL Processing Equipment

Figure 4 reports the simple payback periods (years) for each vessel geometry under three NGL production equipment by dewpointing (Joule–Thomson throttling, turbo-expansion, and mechanical refrigeration). Because the benefit stream is defined as annual retained NGL sales revenue after 7-day storage shrinkage (with no OPEX included, because of the variation of options), these paybacks is interpreted as upper-bound (best-case) capital recovery speeds driven purely by retained revenue.

Across all 15 cases, the payback times fall well below 1 year, ranging from 0.226 to 0.758 years (≈ 2.7–9.1 months). This implies that the associated capital can be recovered solely on a retained-revenue basis.

For each of the three process options, payback increases monotonically in the same order:

Conical < Vertical cylindrical < Horizontal cylindrical < Cuboidal < Spherical:

- Conical is always the fastest-paying configuration: 0.226–0.367 year.
- Spherical is always the slowest: 0.466–0.758 year.

A notable pattern is the near-constant scaling of the geometry effect across the three process options: the spherical vessel's payback is ~2.06× the conical vessel's payback in every column (JT, turbo-expansion, and mechanical refrigeration). It can be deduced that for the JT expansion and mechanical refrigerator production route, the vessel shape effect does "average out" with process selection, unlike the case of the turbo-expansion process.

A sharp rise in the payback penalty of approximately +21, +52, +93, and +106 for the vertically cylindrical vessel, horizontal cylindrical vessel, cuboidal vessel, and spherical vessel, respectively, in production-economics terms, it means that geometry choice materially shifts the capital recovery time because it changes the annual retained sales value of NGL remaining after storage.

Holding vessel type constant, the ordering is also consistent:

Mechanical refrigeration (shortest payback) < Joule–Thomson < Turbo-expansion (longest payback)

- Mechanical refrigeration ranges from 0.226 to 0.466 yr and is the lowest in each vessel row.
- Joule–Thomson ranges 0.255–0.526 yr and sits in the middle.
- Turbo-expansion ranges 0.367–0.758 yr and is the highest in every vessel row.

The relative gaps are uniform across vessel types: turbo-expansion PB (is about 44% longer than JT), while mechanical refrigeration PB (is about 11% shorter than JT). It is observed that the retained-revenue advantage under a simple payback metric has the option for the turbo-expander option capital intensity outweighed; as expected of broader gas-processing knowledge: turboexpanders provide deep refrigeration via near-isentropic

expansion and are widely used to recover valuable liquids, but they are specialized cryogenic rotating equipment within integrated plants.

From a production-economics perspective, the main actionable result is that all configurations pay back within a year on retained-revenue alone, suggesting strong economic motivation to address shrinkage losses.

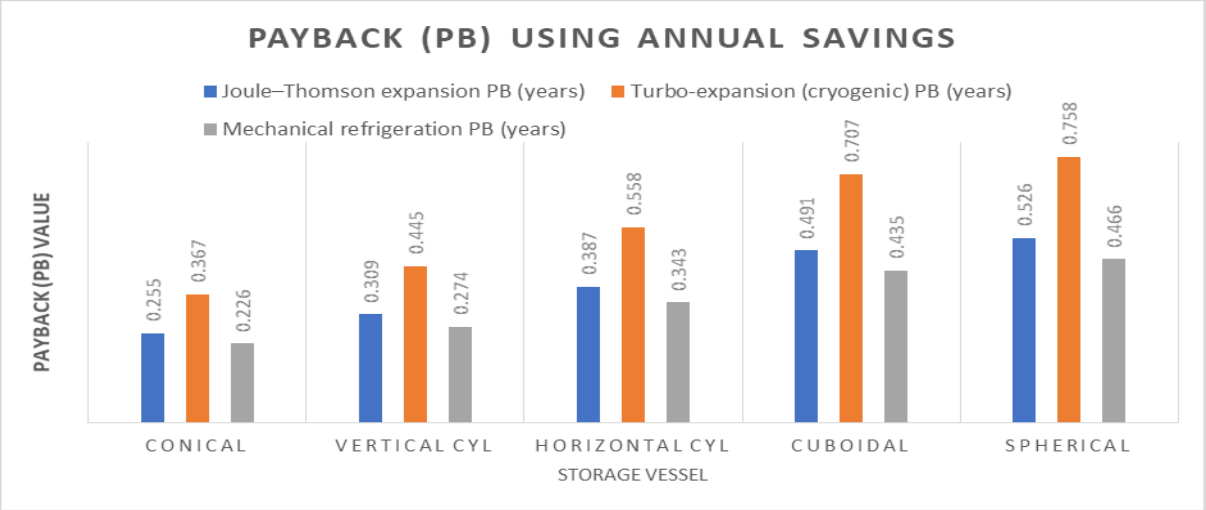

Figure 4. Payback (PB) value for different NGL processing equipment

4.9 ROI as a Loss-amount Index for Annual NGL after Shrinkage

As shown in Table 6, the fraction of annual NGL that was lost after shrinkage (expressed here as ROI_L) varies materially by storage geometry: Conical, Vertical cylindrical, Horizontal cylindrical, Cuboidal, and Spherical vessels, where identified with 61.6%, 68.4%, 74.8%, 80.1%, 81.4% ROI values, respectively. The lower part of Table 6 also shows the retained-yield index relative to the no-shrinkage production baseline. There is a spread of 19.8 percentage points between the best and worst geometries.

In Table 6, ROI_L shows a clear, monotonic ranking in loss NGL, in the order

Spherical ≈ Cuboidal > Horizontal Cyl > Vertical Cyl > Conical.

Relative to conical storage, the improvement in retained fraction is:

- +6.8 pp (vertical cylinder), +13.2 pp (horizontal cylinder), +18.5 pp (cuboidal), and +19.8 pp (spherical).
- Equivalently, a large yield lever of approximately 52% is observed as one moves from conical (38.4% loss) to spherical (18.6% loss), representing an approximate ROI of 52% reduction in shrinkage loss on this basis (18.6 vs 38.4).

Within this framework, vessel geometry acts as a practical proxy for how the system presents heat transfer and mass transfer opportunities over the storage period (e.g., vapor-space behaviours and effective interfacial exposure), which plausibly drives the observed retained-yield differences.

Although labelled ROI, the metric in Table 6 is a retained-production ratio (annual NGL after shrinkage divided by annual NGL before shrinkage). That is distinct from the conventional finance/engineering-economy ROI definition (return relative to an investment outlay), which is typically tied to cash flow and capital.

Table 6: Loss and retained amounts for dew-pointing equipment as CAPEX across the storage vessels: ROI_L (%) for NGL loss in the vessel during shrinkage and ROI_R (%) for NGL retained in the vessel after shrinkage.

Vessel	Conical	Vertical Cyl	Horizontal Cyl	Cuboidal	Spherical
ROI_L (%)	61.60	68.40	74.80	80.10	81.40

Vessel	Conical	Vertical Cyl	Horizontal Cyl	Cuboidal	Spherical
ROI_R (%)	38.40	31.60	25.20	19.90	18.60

4.10 Revenue-to-CAPEX ROI of Dewpointing Options Under Storage-shrinkage Losses

Figure 5 reports the revenue-to-CAPEX screening percentage, defined as the ratio of the annual sales value of NGL retained after shrinkage to the CAPEX of the dewpointing equipment. This is a pre-tax, revenue-based ROI (no OPEX, no depreciation, no discounting), and therefore functions as a screening metric rather than a full investment appraisal. This framing aligns with common "back-of-the-envelope" engineering-economy measures that relate annual cash flow (or savings) to initial investment.

All reported ROIs are well above 100% (≈132% to 443%). This buttresses the previously evaluated short payback time, as the annual retained NGL sales value exceeds the equipment CAPEX for every vessel–equipment pairing.

Figure 5 shows that, for every equipment type, ROI decreases from conical → spherical: as Joule–Thomson (JT), Turbo-expansion, and Mechanical refrigeration show decrease of 392.7% (conical) → 190.1% (spherical), 272.7% (conical) → 132.0% (spherical), and 442.9% (conical) → 214.4% (spherical), respectively.

It is also observed that the conical vessel produces about 2.06× the ROI of the spherical vessel in each column (e.g., 392.7/190.1 ≈ 2.06; 272.7/132.0 ≈ 2.06; 442.9/214.4 ≈ 2.06). This consistency indicates that vessel geometry is acting as a stable multiplier on annual retained revenue, hence on ROI, under the study's shrinkage regime, according to U.S. Environmental Protection Agency (1997), the established tank-loss concepts where evaporative losses (and therefore "retained saleable inventory") depend on storage behaviour and conditions; AP-42 explicitly distinguishes storage ("breathing/standing") and working losses as core mechanisms.

Holding the vessel constant, the ROI ordering is identical for all five vessels:

Mechanical refrigeration ROI (highest) > JT ROI > Turbo-expansion ROI (lowest)

The scale of the difference is also very regular: mechanical refrigeration ROI is ~12–13% higher than JT, while turbo-expansion ROI is ~44% lower than JT across vessels. In a revenue/CAPEX metric, this pattern primarily signals CAPEX intensity differences among the three options (since the retained-revenue driver is anchored in the vessel's shrinkage outcome).

Comparing the NGL recovery process, it is observed that the turbo-expander system is superior in energy efficiency and production cost when the full process context is optimized, rather than judged solely by CAPEX.

Fig. 5 supports the payback analysis, as the same economics are expressed. Here, it is observed that high ROI values indicate that prevention of shrinkage as well as retained sales value can dominate initial equipment cost with the use of conical storage.

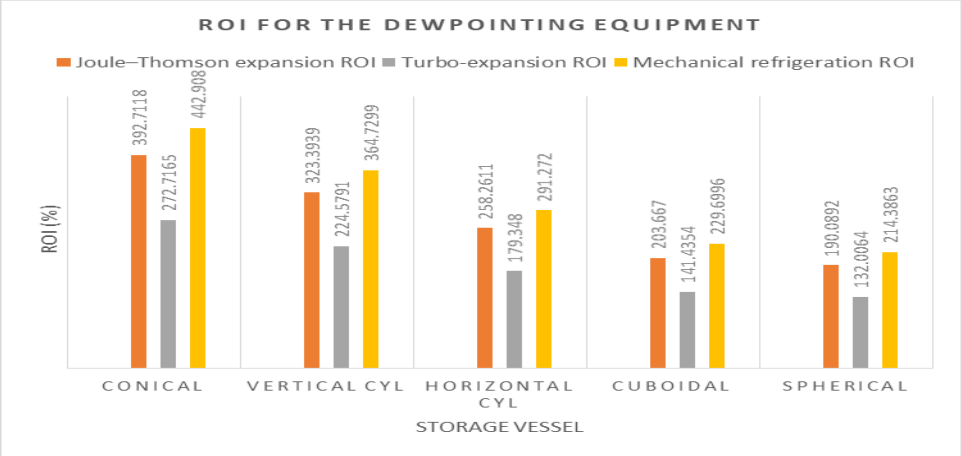

Figure 5. ROI (%) for each equipment option based on annual retained volume of NGL in storage vessels

5. Conclusion

The study was conducted with close observation for seven days, and it was found that NGL shrinkage within the period of study at the short-term apparent shrinkage study, done under bench-scale ambient conditions, was influenced by vessel geometry. Among the evaluated geometries, the conical vessel exhibited the highest volume retention, consistent with its smallest exposed area (36 cm^2). Vessels associated with larger exposed areas, notably the spherical (804 cm^2) and vertical cylindrical (707 cm^2) configurations, showed greater cumulative shrinkage.

The economic implication is that reduced shrinkage produces higher saleable volume and lower value loss. The economic metrics considered in the study provide a practical basis for screening storage options. The findings emphasised that geometry selection can minimize exposed interfacial area and reduce vapor renewal.

This work monitored the shrinkage of NGL over a short period in vessels with scale and geometries characterized by loss volumes and headspaces. Future work should be more general by regularly monitoring temperature and airflow conditions, characterizing NGL composition before and after storage, adding a gravimetric mass balance, and testing sealing and vapor-recovery scenarios. These will give a more comprehensive dataset for production-economic evaluation. In addition, scale-up studies should examine whether the geometry-retention relationship holds when headspace dynamics and thermal gradients differ from bench scale.

CRediT Authorship Contribution Statement

Gideon Mudiaga Efetobor: Writing - review and editing, writing- original draft.

Idongesit Effiong Ekpo: Writing – original draft, investigation, conceptualization.

Ozioma Achugasim: Validation, supervision, conceptualisation.

Pereware Adowei: Investigation, methodology, formal analysis.

Remy Uchachukwu Duru: Writing - review and editing, methodology.

Funding

This research received no external funding.

Conflicts of interest

The authors declare no conflicts of interest.

Data availability

Data are contained in the article and its associated figures and tables. Additional processed data can be made available upon reasonable request.

References

[1] American Petroleum Institute, 2020. API Standard 650: Welded tanks for oil storage (13th ed.). American Petroleum Institute.
[2] American Petroleum Institute, 2021. Manual of petroleum measurement standards (MPMS), Chapter 3.1A: Standard practice for the manual gauging of petroleum and petroleum products (Consolidated version of 3rd ed., incorporating Errata 1).
[3] American Society of Civil Engineers, 2022. Minimum design loads and associated criteria for buildings and other structures (ASCE/SEI 7-22). American Society of Civil Engineers.
[4] Autodesk, 2024. What's new in AutoCAD 2024. Autodesk Help.
[5] Badings, T. S., van Putten, D. S., 2020. Data validation and reconciliation for error correction and gross error detection in multiphase allocation systems. *Journal of Petroleum Science and Engineering, 195*, 107567. https://doi.org/10.1016/j.petrol.2020.107567
[6] de Souza Filho, P. L., de Oliveira, E. C., Aramaki, T. L., 2021. Maximum permissible differences in LPG operations for custody transfer measurements. *Measurement, 175*, 109117. https://doi.org/10.1016/j.measurement.2021.109117

[7] Carlier, J., Papalexandris, M. V., 2024. Turbulent natural convection in an air–water system with evaporation across the free surface. *International Journal of Multiphase Flow, 177*, 104873. https://doi.org/10.1016/j.ijmultiphaseflow.2024.104873

[8] EFFECT4buildings. (n.d.). Guideline for financial calculation methods: EFFECT4buildings toolbox (Annex 2). Interreg Baltic Sea Region / EU Programme. Retrieved March 2, 2026, from https://build-up.ec.europa.eu/sites/default/files/content/2-guideline-for-financial-calculation-methods.pdf

[9] García-G, D., Barco-Burgos, J., Chaparro, J., Eicker, U., Cárdenas, J. D. R., Saldaña-Robles, A., 2024. Analyzing joint efficiency in storage tanks: A comparative study of API 650 standard and API 579 using finite element analysis for enhanced reliability. *International* Journal of Pressure Vessels and Piping, 207, 105113. https://doi.org/10.1016/j.ijpvp.2023.105113

[10] EOG Resources, Inc., 2025. Second quarter 2025 supplemental financial and operating data Tables. https://filecache.investorroom.com/mr5ir_eogresources2/418/Tables_for_Website_08-07-25_dated_08-06-25.pdf

[11] Huang, W., Wang, S., Jing, H., Wang, C., Sun, X., Zhou, N., Fang, J., Fu, L., 2020. A calculation method for simulation and evaluation of oil vapor diffusion and breathing loss in a dome roof tank subjected to the solar radiation. *Journal of Petroleum Science and Engineering, 195*, 107568. https://doi.org/10.1016/j.petrol.2020.107568

[12] International Organization for Standardization, 2022. ISO 7507-2:2022 Petroleum and liquid petroleum products—Calibration of vertical cylindrical tanks—Part 2: Optical-reference-line method or electro-optical distance-ranging method (3rd ed.). ISO.

[13] International Organization for Standardization. (2023). ISO 4266-1:2023 Petroleum and liquid petroleum products—Measurement of level and temperature in storage tanks by automatic methods—Part 1: Measurement of level in atmospheric tanks (2nd ed.). ISO.

[14] Jindamanee, K., Keawboonchu, J., Pinthong, N., Meeyai, A., Inchai, P., & Thepanondh, S. (2025). Environmental impacts and emission profiles of volatile organic compounds from petroleum refineries. *Scientific Reports, 15*, 15509. https://doi.org/10.1038/s41598-025-99932-7

[15] Lake, T. (n.d.). Return on investment (ROI). Britannica Money. Retrieved March 2, 2026, from https://www.britannica.com/money/return-on-investment

[16] Mansour, E. M., El Aily, M., & Desouky, S. M. (2020). Flashing losses emission evaluation from crude oil storage tanks. *Egyptian Journal of Chemistry, 63*(11), 4457–4462. https://doi.org/10.21608/EJCHEM.2020.24509.2467

[17] National Renewable Energy Laboratory (n.d.) 2026. Payback period (System Advisor Model documentation). Retrieved March 2, 2026, from https://samrepo.nrelcloud.org/help/mtf_payback.html

[18] Noaman, A., Ebrahiem, E. E., 2021. Comparison of Natural Gas Hydrocarbon Dewpointing Control Methods. Journal of Advanced Engineering Trends 40(2):99-116. DOI:10.21608/jaet.2020.31288.1020

[19] Orsay, G. L., & de Oliveira, E. C. (2025). Robust approach connected to measurement uncertainty for establishing acceptance limits in custody transfer measurements within the oil and gas industry. *Chemical Engineering Science, 318*, 122248. https://doi.org/10.1016/j.ces.2025.122248

[20] Poós, T., Varju, E., 2020. Mass transfer coefficient for water evaporation by theoretical and empirical correlations. International Journal of Heat and Mass Transfer, 153, 119500. https://doi.org/10.1016/j.ijheatmasstransfer.2020.119500

[21] Shabani, A., Maroti, G., de Leeuw, S., Dullaert, W. (2021). Inventory record inaccuracy and store-level performance. *International Journal of Production Economics, 235*, 108111. https://doi.org/10.1016/j.ijpe.2021.108111

[22] Shamsi, M., Obaid, A. A., Vaziri, M., Mousavian, S., Hekmatian, A., & Bonyadi, M. (2024). A comprehensive comparison of the turbo-expander, Joule-Thomson, and combination of mechanical refrigeration and Joule-Thomson processes for natural gas liquids production. Energy, 295, 131032. https://doi.org/10.1016/j.energy.2024.131032

[23] Shoghl, S. N., Naderifar, A., Farhadi, F., Pazuki, G., 2022. A novel strategy for process optimization of a natural gas liquid recovery unit by replacing Joule–Thomson valve with supersonic separator. Scientific Reports, 12, 22398. https://doi.org/10.1038/s41598-022-26692-z

[24] Tabari, M. R. R., Sabzalipour, S., Peyghambarzadeh, S. M., & Jalilzadeh Yengejeh, R., 2020. Determining the emission rates of volatile organic compounds and modeling their dispersion from the petroleum and chemical storage tanks of the largest oil terminal in the southwest of Iran. Journal of Advances in

Environmental Health Research, 8(4), 269–280. https://doi.org/10.22102/jaehr.2021.251979.1187

[25] The Open University. (n.d.) 2026. Relevant cash flows and sunk costs (Challenges in advanced management accounting, Section 3.1). Open Learn. Retrieved March 2, 2026, from https://www.open.edu/openlearn/money-business/challenges-advanced management-accounting/content-section-3.1

[26] U.S. Energy Information Administration. (2023a, December 26). Hydrocarbon gas liquids explained. U.S. Energy Information Administration. https://www.eia.gov/energyexplained/hydrocarbon-gas-liquids/

[27] U.S. Energy Information Administration. (2023b, December 26). Transporting and storing hydrocarbon gas liquids. https://www.eia.gov/energyexplained/hydrocarbon-gas-liquids/transporting-and-storing-hydrocarbon-gas-liquids.php

[28] U.S. Environmental Protection Agency. 1997. *AP-42: Compilation of air pollutant emission factors, Chapter 7—Liquid storage tanks, Section 7.1 Organic liquid storage tanks* (5th ed.). https://gaftp.epa.gov/ap42/ch07/s01/final/c07s01.pdf

[29] U.S. Environmental Protection Agency. (2020, June). *AP-42: Compilation of air pollutant emission factors (5th ed.), Volume I: Stationary point and area sources—Chapter 7, Section 7.1: Organic liquid storage tanks* (Final section—June 2020 error corrections). https://www.epa.gov/sites/default/files/2020-10/documents/ch07s01.pdf

[30] U.S. Environmental Protection Agency, 2023. Inventory of U.S. greenhouse gas emissions and sinks: 1990–2021 (Annexes). U.S. Environmental Protection Agency. https://www.epa.gov/ghgemissions/inventory-us-greenhouse-gas-emissions-and-sinks

[31] U.S. Energy Information Administration. (2024, October 10). Natural gas explained. U.S. Energy Information Administration. https://www.eia.gov/energyexplained/natural-gas/index.php

[32] U.S. Energy Information Administration. (n.d.) 2026. *Propane prices: Mont Belvieu, Texas (WPROPANEMBTX)* [Data set]. FRED, Federal Reserve Bank of St. Louis. Retrieved February 23, 2026, from https://fred.stlouisfed.org/series/WPROPANEMBTX

[33] Varju, E., Poós, T., 2022. New dimensionless correlation for mass transfer at evaporation of open liquid surface in natural convection. *International Communications in Heat and Mass Transfer, 136*, 106102. https://doi.org/10.1016/j.icheatmasstransfer.2022.106102

[34] Verret, J., Qiao, R., and Barghout, R. A. (2024, May 22). 6.2: Purchased equipment (PE) **cost**. In *Foundations of Chemical and Biological Engineering I*. *Engineering LibreTexts*. Retrieved February 23, 2026, from https://eng.libretexts.org/Bookshelves/Chemical_Engineering/Foundations_of_Chemical_and_Biological_Engineering_I_(Verret_Qiao_Barghout)/06%3A_Process_Economics/6.02%3A_Purchased_Equipment_(PE)_Cost

[35] Vipond, T. (n.d.) 2026. Return on investment: Formula, meaning, and how to calculate it. Corporate Finance Institute. Retrieved March 2, 2026, from https://corporatefinanceinstitute.com/resources/accounting/return-on-investment-roi-formula/

[36] Zinke, R., Köhler, F., Klippel, A., Krause, U., Leitl, B., 2020. Emissions of volatile hydrocarbons from floating roof tanks and their local dispersion: Considerations for normal operation and in case of damage. *Journal of Loss Prevention in the Process Industries, 66*, 104179. https://doi.org/10.1016/j.jlp.2020.104179